Depth dependence and intra-tidal variability of Suspended Particulate Matter transport in the East Anglian plume

Meinard C.H. Tiessen[a,b], Marieke A. Eleveld[c,b], Janine J. Nauw[d], Bouchra Nechad[e], Theo Gerkema[a]

[a] *NIOZ Netherlands Institute for Sea Research, Department of Estuarine and Delta Systems, and Utrecht University, P.O. Box 140, 4400 AC Yerseke, The Netherlands*
[b] *Deltares, P.O. Box 177, 2600 MH Delft, The Netherlands*
[c] *Vrije Universiteit Amsterdam, Institute for Environmental Studies (VU-IVM), De Boelelaan 1087, 1081 HV Amsterdam, The Netherlands*
[d] *NIOZ Netherlands Institute for Sea Research, Department of Coastal Systems, and Utrecht University, P.O. Box 59, 1790 AB Den Burg, The Netherlands*
[e] *Royal Belgian Institute of Natural Sciences, ODNE, Gulledelle 100, 1200 Brussels, Belgium*

Abstract

In order to derive an estimate of the net transport of Suspended Particulate Matter (SPM) in the East Anglian plume, we carried out a measurement campaign along two cross-sections within the plume. Selected stations were visited repeatedly to resolve the tidal cycle. By measuring profiles of currents and optical backscatter (from which SPM concentrations were estimated, via samples), both gross and net transports can be calculated, as well as intra-tidal and vertical variability. For the center of the plume, we find a net transport of about 13 million kg over a tidal cycle. A comparison is made with maps of near-surface concentration of SPM from optical remote sensing. Some discrepancy is found in the values (of about a factor of two), but the spatial pattern agrees qualitatively.

Keywords:

SPM, transports, North Sea, tidal currents, remote sensing

Highlights:

- An observation based estimate of transport in the East Anglian plume yields a net eastward transport
- Within a tidal cycle, both stratification and the SPM concentration profiles vary strongly in the East Anglian plume
- Residual transports of SPM are calculated for the center of the plume
- In-situ measurements and remote sensing correspond qualitatively, but the latter is lower by about a factor of two.

---

1. Introduction

The East Anglian plume forms one of the pathways of suspended particulate matter (SPM) in the Southern North Sea (Dyer and Moffat, 1998). In Figure 1a, the plume is visible by its relatively high concentrations of SPM at the surface, as observed by remote sensing. It leaves the East Anglian coast across the Norfolk Banks and then follows more or less an eastward direction along the Terschellinger Bank and the Frisian Front, in a range of water depths between about 30 and 40 meters.

This frontal area is special in several ways. During summer, it marks the transition between well-mixed conditions to the south and stratification to the north (Pingree et al., 1978); a more detailed view was obtained from modelling results by (van Leeuwen et al., 2015). In terms of bed composition

in the southern North Sea, it forms the boundary between a generally low-silt content ($< 2\%$) to the south, and high silt content ($> 10\%$) to the north (Creutzberg and Postma, 1979), although sediment composition on the North Sea floor also shows a lot of patchiness due to its complex development during the Pleistocene (Eisma, 1987). Finally, the plume follows the general direction of the circulation (Otto et al., 1990), reflecting the presence of frontal jets (Hill et al., 2008); these flows show some variation with wind strength and direction (Nauw et al., 2015).

The overall distribution of suspended matter concentrations in the southern North Sea is known from extensive in-situ measurements, see, e.g., Eisma and Kalf (1987b). For surface values, optical remote sensing provides detailed maps, in which the East Anglian plume is often clearly visible (Eleveld et al., 2008; Pietrzak et al., 2011). SPM concentrations in the southern North Sea are persistently high at the head of the East Anglian plume, near the Humber Estuary, over the southern edge of the Norfolk Banks, and in the Greater Thames Estuary. Along the Belgian and Dutch continental coast, year-round high SPM concentrations occur over the Flemish Banks, and near the Wadden Sea and Weser-Elbe Estuary (Eleveld et al., 2008). Along both the shallow UK and the continental coasts ample fine sediment is available for resuspension by strong tidal currents from both older deposits and recent supply; besides, river discharge is a factor (de Jonge and de Jong, 2002).

The East Anglian plume crosses the North Sea from southeast England and occasionally even extends northward past the Dutch Wadden Sea and offshore from the Danish coast, most clearly so in October to March (Eleveld et al., 2008). In these months, surface SPM concentrations in the East An-

glian plume are influenced by winds and waves in addition to tides; they produce increased advection and sufficient shear stress to also resuspend mud from the deeper (> 35 m) regions (Pietrzak et al., 2011, Fig. 8) to the top of the well-mixed water column, where it can be detected with satellite sensors. In a modelling study, Stanev et al. (2009) also found wave-induced shear stress to be significant for resuspension at these deeper locations, besides current-induced shear stress, although there are additional factors, such as the local bottom composition.

The sources and sinks of fine sediment in the North Sea have been broadly identified (see Dyer and Moffat, 1998, for a short overview). In particular, Dyer and Moffat (1998) made an estimate of the total net eastward transport of SPM in the East Anglian plume by multiplying the residual current (obtained from a numerical model) with the depth-average SPM concentration. Their estimate was 6.6 megatons/year, with, however, an error range of 50%. We are not aware of studies on the fate of the SPM in the East Anglian plume, but given the general direction of the plume, the major deposition areas of the Kattegat and Skaggerak (Eisma, 1987) are likely candidates.

In this study, we calculate transports according to their actual definition, namely by multiplying instantaneous currents u (in m/s) and concentrations c (in g/m^3) at individual positions in the vertical, and then integrate this product over time and over the area of the transect. (Notice that, in principle, the resulting transport may even be opposite to the residual current.) Moreover, our estimates are purely observation-based; we are not aware of similarly obtained earlier estimates for the East Anglian plume.

We consider the transport of water and SPM that occurs within a tidal

period. Intensive measurements are needed to determine instantaneous current and concentration profiles throughout a full tidal period. The aim of this research is to identify the transport rates of SPM along this plume, and investigate variability in the vertical and with time (specifically the tidal cycle), across and along the plume. We start with an overview of the area and methods in Section 2. In Section 3, we present measurements made along two transects (T1 and T2), for each one a detailed spatial coverage was followed by repeated measurements at selected stations over a tidal cycle. Extensive measurements of current profiles, optical backscatter (OBS) and SPM concentrations allow us to establish a relationship between OBS and SPM, and hence to calculate the gross transports of SPM during the ebb and flood phases of the tidal cycle, as well as the net result over a tidal cycle. In Section 4, we compare near-surface values of SPM from in-situ measurements with estimates from optical remote sensing.

2. Measurements

2.1. Research area and cruise plan

The cruise took place on board NIOZ R/V Pelagia, from 6 to 15 March 2013 (days of year 65-74). We carried out in-situ measurements at two transects across the plume, indicated by the blue lines in Fig. 1. The first transect (T1) lies in the middle of the Southern Bight, spanning from 52°54.0′N 3°15.0′E to 53°53.4′N 3°15′E. The location was determined using a map of surface values of SPM estimated from a remote-sensing image from the 4th of March (day of year 63), two days prior to the start of the cruise, see Fig. 1a.

The SPM maps were produced from the Level-1 images acquired by the Moderate-resolution Imaging spectroradiometer (MODIS) onboard of the NASA spacecraft Aqua. These data, processed by the Ocean Biology Processing Group, are available from the NASA Ocean Color website (`http://oceancolor.gsfc.nasa.gov`). The Level-1 images were then atmospherically corrected using the near-infrared atmospheric correction algorithm implemented in the SeaDAS software, yielding images of water-leaving reflectance (ρ_w). Finally, SPM concentration is retrieved from ρ_w data at band 667 nm, using the algorithm of Nechad et al. (2010). The algorithm is applied here because 1) this semi-empirical model has been calibrated and validated using measurements taken in the southern North Sea (2001-2006), and 2) it is designed for use in the case of turbid waters (SPM>1 mg/l, up to SPM 100 mg/l). The choice of this algorithm using band 667 nm has the advantage to estimate SPM concentrations with the best accuracy from MODIS band 667 (relative error<30%). For the 1-200 mg/l concentration range, this band has a higher signal-to-noise ratio than the longer infrared bands, while the significant contributions from CDOM and Chl absorption to reflectance at shorter wavelengths can lead to larger uncertainties in SPM retrieval. The disadvantage is that estimation of SPM from band 667 nm may show larger uncertainties (>33%) in the case of extreme chlorophyll concentrations (>10 μg/l), but this effect should be reduced for the East Anglian plume in March; the mean seasonal Chl concentrations from 1988 to 2011 range between 1 and 7μg/l approximately (Capuzzo et al., 2015).

The image in Fig. 1a shows a relatively wide but low-intensity plume, beyond the initial higher SPM concentrations close to the UK coast. The

second transect (T2) was located at the eastern edge of the plume, from 53°24.0′N 5°9.0′E to 54°15.6′N 4°10.9′E. Later remote-sensing images are also shown in Figures 1b-d; they will be discussed in Section 4.

The main objective is to determine the vertical and intra-tidal variability in SPM concentration and transport rates in the East Anglian plume. In initial surveys, measurements were conducted to locate the centre of the plume, where concentrations are highest. For T1, this survey was carried out on the 7th of March (day of year 66), and for T2 on the 12th of March (day of year 71). In the ensuing days at each transect, more detailed measurements would follow by repeatedly visiting selected stations near the centre of the plume. This involved measurements over a 14-hour period, to resolve the variability in SPM dynamics over a tidal cycle; additionally, longer transects were conducted to monitor the location and width of the central part of the East Anglian plume.

The high-frequency measurements included either two or three stations, at a distance of 5 km from each other. Measurements were then conducted every 45 minutes at a different station. For a 2-station session, this means that every 1.5 hours each station was visited, resulting in 10 or 11 data-points during a 14-hour period. When three stations were included during a day, the central station would be visited every 1.5 hours, and the outside stations only every 3 hours. These outside stations were however visited more frequently (10 or 11 times during the 14 hour session) during the previous or ensuing day (see Tiessen, 2013, for the detailed cruise program).

New Moon was on 11 March and the strongest currents (according to the Oregon State University model) occur about two days later in this area.

At spring tides, maximum currents in the east-west direction are similar for both transects (according to the model), but the tidal cycles were covered on different days: on 8 March for T1 and 14 March for T2. So, for T1, the condition was in between neap and spring tides, whereas T2 was right after spring tides. This is confirmed by Figures 5e,f, where currents are stronger in the latter. Regarding the diurnal inequality (again according to the model), for the eastward component at T1, the maximum flood just prior to the measurements was equal to the one at the end of the measurements. For T2 on 14 March, the second flood (right after the measurements) was only slightly higher (a few cm/s). In short, the diurnal inequality does not seem to play an important part here; the beginning and end of the measurements closes a nearly periodic cycle.

Weather conditions during the cruise were variable: mild conditions were experienced prior to departure as well as during the first day of the cruise, which was mainly spent in transit. Subsequently, cold weather and strong easterly to northeasterly winds persisted during the first half of the measurement campaign, but the wind dropped considerably during the second half of the cruise and turned northerly to northwesterly. Fig. 2 shows the wind conditions as recorded during the first half of March 2013. Wind conditions during the cruise are taken from ship records, whereas data prior to the cruise is from the KNMI weather station Terschelling. (Comparison of the two during the cruise, not shown here, indicates that wind speeds recorded on the ship are slightly higher than those at the weather station; this is due to two factors: the lack of obstruction at sea and a higher location of the wind sensors onboard of the ship.) Measurements were conducted along T1

during days of year 66 to 70, and along T2 during days of year 71 to 73. The strong (north)easterly winds therefore coincided with the measurements conducted along T1, whereas the milder northerly to northwesterly winds prevailed during the measurements along T2.

2.2. Equipment and methods

Vertical profiles of temperature and salinity were made by lowering and hoisting a CTD frame containing a SBE3 plus thermometer and a SBE4 conductivity sensor as well as a Seapoint OBS and a rosette with three 8-liter Niskin bottles. In the post-processing, the data was binned to 1 m vertical intervals. A Workhorse Monitor 300 kHz ship-mounted ADCP was used with a bin size of 1 m and had profiles recorded every 60 seconds.

During each visit to a station, vertical profiles were taken with the CTD and OBS. The former produces profiles of temperature and salinity. The OBS provided proxy-measurements of the SPM concentration. To link them, water samples were collected (using 8-liter Niskin bottles) at each station at three depths (1 m above the bottom, halfway down the water column, and 1 m below the surface). These water samples where filtered (over dried and pre-weighed GF/F filters) and subsequently (back at the institute) dried and weighed to obtain the SPM concentration at the different moments, depths, and locations. Separately, in the lab on board the ship, OBS values were obtained from the same water samples. This provides us with a relation between OBS values and SPM concentrations, shown in Fig. 3, for the separate transects (brown for T1 and green for T2). The scatter in the plot can reflect variations in the OBS response, which depends on factors like organic content, particle shape, color and flocculation (Downing, 2006). Linear fits

are shown for the separate transects as well as for all data points combined (black dashed line). For T1 and T2, the slopes are different, but so are the intercepts; the result is that for the large majority of points (concentrations lower than 40 mg/l), the lines are actually close. However, for T2 there are only very few points at large OBS values, so that the line is mainly based on the cloud of points in the lower left corner. To translate OBS profiles into SPM profiles, we therefore used the combined data (SPM=2.8+1.83*OBS). The root mean square error is 5.5 mg/l, which is 30% of the median concentration of 18.2 mg/l. We take this to be the plausible range of error for the transports (calculated below).

At each station, ADCP data was selected from a 10-minute interval, starting two minutes before the CTD-profile was made; in all cases, the duration of making the CTD profile fell well within this interval. Single velocity profiles were then constructed by taking the median value for each bin from the 10-minute interval.

The CTD-casts recorded the water depth and bed level, relative to the tidal elevation, for each visit to a station. We assume that the bed-level was nearly constant in the small area surrounding each station, within which the profiles were taken. The water depth recorded by the CTD is thus taken as measure for the bed-level and tidal elevation for the different stations. The bed-level recorded during each CTD-cast is also taken as the reference value for the current profile, obtained by the ADCP-sensor. Side-lobe interference reduces the accuracy of ADCP measurements near the seabed. As a result, the data of the lowest 10% of each ADCP-profile were ignored. A power-law was fitted to the four data points nearest to the bed to obtain the currents

in the lowest part of the water column. ADCP-profiles also lacked data close to the surface, due to the blanking distance (1.76 m) and the depth at which the ADCP was mounted (3.6 m). To fill this gap, we assume that currents remain constant towards the surface and thus apply a constant extrapolation based on the average of the four data-points nearest to the surface.

3. Results

3.1. Plume distribution

The initial survey at each of the transects reveals a distinct distribution, both with respect to the different water masses and to the location of the SPM plume. Along T1 (conducted on March 7th, day of year 66), the transition from the warmer and more saline English Channel water to the water mass of the Central North Sea can be observed in Fig. 4ac, showing the temperature and salinity distributions. This is in line with earlier observations, such as shown in Otto et al. (1990) for the month of February, where tongues of warmer saline water are seen to enter via the Channel and the Atlantic in the northern North Sea (see also Nauw et al., 2015), enveloping the colder fresher water in the Central North Sea and along the coasts in the Southern Bight (Pietrzak et al., 2011). In the frontal area between the two water masses (which spans roughly 50 km), the highest SPM concentrations occur (Fig. 4e). The plume is very patchy, though; also profiles are found with very low SPM concentrations, in particular near the surface. This suggests that there are local patches of resuspension. Based on the data obtained during this first survey, as well as on data from similar albeit shorter transects in the ensuing days, the stations ranging from latitude 53.35 to 53.62°N were examined over

various tidal cycles to determine inter- and intra-tidal variability.

For the second transect (T2), a similar initial survey as for T1 was conducted to determine the centre of the SPM plume on March 12th (day of year 71). This was a necessary verification of whether the location of the plume was still similar to the one indicated by the earlier satellite image of March 4th; the change in weather conditions might have shifted the location of the plume, while cloud cover inhibited more recent satellite images to be inspected. Fig. 4bd shows that along this transect, too, a transition between water masses occurs. The northern part of the transect still features Central North Sea Water and just south of it, we find warmer more saline water from the Channel. But now, in the southern part of the transect, there is an additional third water mass: fresh cold water indicating the presence of the Rhine plume along with freshwater sources from the Wadden Sea. The transition between the last two water masses shows a distinct vertically stratified area, where the fresher water lies on top of the Channel water. The plume, with SPM concentrations of typically 10-15 mg/l (Fig. 4f), is located in this transition zone. The highest concentrations are found at stations where no stratification occurs, whereas the stratified profiles indicate a faint SPM plume extending offshore underneath the fresher top layer. Clearly, the SPM is largely restricted to the lower layer whenever stratification occurs.

3.2. Intra-tidal variability

Stations located in the centre of the plume were visited repeatedly over at least one tidal cycle, to determine tide-related variability in hydro- and SPM dynamics. Detailed results are here shown for two representative stations, indicated by triangles in Fig. 4, one for each transect. In Fig. 5, following the

panels from top to bottom, we show the density anomaly (i.e., the density minus 1000), the SPM concentration, along-plume current velocities, and cross-plume current velocities. Notice that along-plume currents are defined as being normal to the transect, while cross-plume currents are along the transect.

The density anomaly plot for the station on T1 shows that water masses shift back and forth over a tidal cycle, with more dense water being measured during the later stages of the 14-hour measurement period. Northward directed currents (indicated in red in Fig. 5g), transport the more saline English-Channel water towards the north during that half of the tidal cycle. Throughout the tidal cycle, the highest SPM concentrations are located near the bottom. Overall, the SPM concentrations are significantly higher than those recorded during the initial survey of the entire transect (Fig. 4e), probably due to stronger winds and the resulting higher waves (Fig. 2). Notice that the horizontal current velocity components are out of phase, so that "slack tide" cannot be unequivocally defined, as it occurs at different times for the two components. The peak SPM concentrations occur around the peak of the along-plume current, when directed to the east (Fig. 5e), shown in red).

For T2, the different water masses are separated in the vertical, with only a brief period in the middle of the 14-hour session when stratification is weaker (Fig. 5b). SPM concentrations are much lower than those recorded at T1 and are restricted to the area close to the bottom when the water column is stratified. A faint increase in SPM concentration can be observed when the stratification disappears. This happens during slack, at the end of the east-

and northward flow; Figure 4b,d indicates that vertically mixed water would have moved in the direction of the station, which suggests that the transition from stratified to mixed conditions in Figure 5b can be ascribed to advection. As T2 is located close to the coast, the tidal motion clearly shows periods of peak and slack currents, its polarization being almost rectilinear. The main tidal movement is more or less along the plume, transporting water and SPM along the main axis of the East Anglian plume. However, a direction of net transport is not evident from the figure.

3.3. Net transport rates

In order to determine the transport rates of water and SPM across and along the plume, we proceeded as follows. First, the SPM flux was calculated by multiplying instantaneous current velocities with SPM concentrations, for every 'bin' in the vertical. We note that higher SPM concentrations close to the bed (as shown in Fig. 5cd) do not necessarily result in high SPM fluxes, since the flow velocities are small there. The fluxes were then vertically integrated, resulting in the values shown as open circles in Fig. 6. This forms the time-series at one specific station on T1 (Fig. 6, left panels) and T2 (right panels).

For T1 the transport is more asymmetric than for T2. For T1, the eastward transport, during the last phase of the cycle in Fig. 6a, is significantly higher than the westward transport during earlier phase. For T2, the evolution is more symmetric (Fig. 6b). Moreover, the along-plume and cross-plume gross SPM transports are for T1 of similar magnitude (compare Fig. 6ac), whereas for T2, the along-plume transport is significantly higher than the cross-plume one (compare Fig. 6bd). This can be directly related to the

characteristics of the tidal current (more circularly polarized for T1, more rectilinear for T2).

With measurements lasting around 14 hours for each station, the results were interpolated to 5-min intervals and then the first 12.4 hours were taken to represent a full tidal cycle. We notice that there is some ambiguity in the definition of the tidal cycle and hence in its duration; this problem was analyzed by Duran-Matute and Gerkema (2015) in relation to residual flows. They showed that although individual periods may vary considerably, also depending on the definition used, the long-term mean tidal period is precisely the M2 period in areas where the M2 is the dominant constituent; this is irrespective of the definition that is adopted. For simplicity, we take this long-term mean value as the tidal period. We then perform a harmonic analysis, extracting the semidiurnal tide (taken to be the principal lunar constituent M2 constituent), the quarterdiurnal tide (M4), and a time-independent constituent (i.e., residual). The sum of these three constituents is represented by a red line in Fig. 6, which in each case closely follows the original values (open circles).

The resulting tidal mean transport, for water and SPM, is shown in Fig. 7 for T1. This tidal-mean (net) transport is shown in black circles. Besides, we also show the gross transports, for the ebb and flood phases, calculated by separately summing the negative and positive contributions of the transports during the tidal cycle, respectively. The sum of the two is the net transport. At most stations, the net transport is significantly smaller than the gross transports during ebb or flood. Nevertheless, for the full transect, the net transport in the along-plume direction of both water and SPM (black circles

in Fig. 7ac) is substantial in the centre of the plume (between latitudes 53.4-53.55°N) and directed towards the east. Outside of this central part, fluxes are generally smaller: further south, transports dwindle, whereas they turn westward in the northern part of the transect. The size of the circles in Fig. 7 is indicative of the number of visits to the station; the more visits, the higher the resolution of the tidal cycle and hence the more reliable the result. For T2, most stations were visited less frequently, and less stations were involved, so they do not provide a sufficient basis for reliably calculating spatially and temporally integrated transports. For this reason, we henceforth focus the discussion on T1.

By integrating along the transect, we calculate the amount of SPM that crosses the transect in a tidal period. For T1, we find an amount of 13 million kg of SPM. Regarding the error estimate belonging to this value, several factors need to be considered. First, this net value is the aggregate of many data points, due to integration in time and space. This means that random errors in individual data points will largely cancel in the aggregate. This is expected to be the case for measurements on current velocities. There are also errors due to lack of resolution in space and time, but they cannot be estimated from our data. Finally, there are possible systematic errors which will affect the net value. A primary example here is the translation of OBS values into SPM concentrations (Fig. 3). As discussed in Section 2.2, the linear fit involves a root mean square error which is about 30% of the median concentration, so we take this as a plausible margin of error for the gross and net transports.

In terms of annual values, this would mean an eastward transport of 9

Megatons per year, which is somewhat more than the amount estimated by Dyer and Moffat (1998), 6.6 Megatons per year, but falls easily within their error estimate of 50%, and ours. Their estimate involved two approximations, for they calculated the transport by multiplying the net water flux (from a model) with depth-averaged SPM concentrations. This would correspond to the exact definition only if the concentration were uniform in space and time. From our results in Fig. 7ab, comparing the black circles in each, it appears that we can indeed regard the net SPM transport approximately as the net water transport times a constant multiplication factor. This factor is the typical concentration, in our case 18 mg/l (median value). This, then, seems to be the main origin of the difference from the results by Dyer and Moffat (1998), for their mean concentrations are typically lower. Their measurements covered a large part of the North Sea (whereas we have zoomed in on the East Anglian plume) and as result, they may have missed the area of high concentrations, which is fairly localized. On the other hand, with a view to yearly transports, their measurements were more comprehensive as they included seasonal differences, whereas in our case it is a bold step to extrapolate the results from just one tidal cycle to a yearly transport. The validity of such an extrapolation depends on how representative this particular tidal cycle was. As argued in Section 2.1, the tidal conditions were in between spring an neap tides and showed no strong diurnal inequality. However, the strong easterly winds would have reduced the westward transport of SPM. In this respect, one can argue that the real annual transport is likely to be higher than our estimate. The same is true in view of the expected higher organic content later in the year, which would enhance SPM concentrations

and hence the transport.

4. Comparison between remote-sensing and in-situ observations

Many processes act to bring particulate matter into suspension or causing it to settle, modifying the colour of the water masses. The original cruise-plan was designed based on satellite data providing insight into the position and spread of the East Anglian plume. Cloud-free conditions led to a detailed and accurate image of the pre-cruise conditions (shown in Fig. 1a). The positioning of transect T1 was based on the most western location where it would still be possible to cover the entire plume's width in a 100 km stretch, and to identify a narrow band of high SPM concentrations consisting of a limited number of stations (5 km spaced apart) that could be visited frequently during a tidal cycle. Transect T2 was determined as being approximately at the end of plume, at that moment.

Subsequent windy weather conditions (see Fig. 2) led to changes in the SPM plume's intensity and location, but this could only be observed afterwards, when weather conditions allowed satellites to observe the water surface again, or at least partially, see Fig. 1b-d. During this period, snowfall and cloud cover prevented satellite images to cover the entire Southern Bight of the North Sea, and additionally the edges of cloud cover contributed to additional random noise to the estimated SPM concentration distribution. However, in Fig. 1c it can be seen that along the English coast, the East Anglian plume intensified and broadened. Where prior to the storm (Fig. 1a) only a patchy plume was observed, it has now become a continuous area with high SPM concentrations. The central part of the plume (where tran-

sect T1 was located) can only be seen partially in the satellite images on the different post-storm days. Here the plume also seems to have intensified, but location and width cannot be clearly deduced from these images. Finally, Fig. 1b shows a more distinct plume along transect T2 than was observed prior to the storm (Fig. 1a). The plume has intensified considerably, and also a clear southward shift has occurred, with the East Anglian plume now almost overlapping with the high SPM concentrations close to the Wadden Sea area.

In order to compare values derived from remote sensing with in-situ observations, a direct comparison is presented in Fig. 8. Here the small dots indicate values derived from satellite imagery, in an area around both transects (with a range off about 10 km), whereas the in-situ measured data is shown in big circles. The latter is derived from the OBS data as the average of the top 4 m below the water surface. The colour of the dots corresponds with the time (in day number) when the measurements were taken. This information is necessary for comparing in-situ and remote sensing estimates in a meaningful way, as this requires a near simultaneity. Measurements along transect T1 were conducted leading up to (shown in blue) and during the bad weather period (green), while transect T2 was sampled during the post-storm period, shown in red. The coloured lines represent a median of the remote-sensing values (shown as the small dots) at the same latitude. The comparison between in-situ and remote sensing data focusses on the pre- (blue) and post-storm (red) periods, when also satellite imagery was available.

During the cruise, stations at the transects were visited several times, as

described above, but in addition higher sampling measurements were conducted at a few individual stations over a tidal cycle (visible in Figure 8 as multiple, vertically stacked, coloured circles at the same latitude) . The first day at each transect, the entire transect was sampled, which provides information most similar to the analysis of satellite images. Overall, a comparison shows that the in-situ measurements give an SPM concentration that is roughly twice as high as the ones derived from satellite images. Bias may occur because the colour (optical properties) of SPM may vary within the North Sea (Tilstone et al., 2012); a detailed validation (Lee (ed.), 2006) would be needed to conclude more about this. Here we put forward several more reasons that may account to a varied degree for these discrepancies, both with regard to the cruise data (as discussed above) and the satellite observations.

Firstly, the satellite images do not exactly match the timing of the cruise data for the pre-storm conditions, as these data mainly originate from day 63, whereas the measurements during the cruise started on day 66. In the meantime, wind conditions had changed in direction and strength, picking up from day 65 (see Fig. 2). This can have a significant effect on the position of the plume and hence on the local intensity of SPM, especially as the plume on day number 63 still showed a locally variable and patchy SPM distribution. However, this explanation does not apply to the post-storm measurements which were conducted during days 71 to 73. Another complicating factor is that the satellite images were taken on a fixed time each day. In contrast, the cruise data showed that the variability in SPM concentration over a tidal cycle can be very significant, as shown in Fig. 5. Finally, we are comparing

surface values, but the very meaning of "surface" may be different for remote sensing, being approximately sensitive to the upper one meter in this area, while in-situ samples were typically taken just below this layer. An extensive comparison was made by Fettweis and Nechad (2011), who also found that SPM values based on remote sensing were lower than those from in-situ measurements.

Overall, we conclude that the spatial trend agrees well between both sets of measurements, while values may differ by a factor of about two.

5. Discussion

Organic content was not measured during this cruise. According to Eisma and Kalf (1987a), the organic content in suspended matter is typically 10-20% in winter. By mid-March, there may already be the beginning of a phytoplankton bloom (as shown by the seasonal cycle in Bale and Morris (1998)); however, March 2013 was unusually cold in northwestern Europe, so organic content is likely to have stayed close to the typical winter values. Another point is that a clear tidal cycle in SPM concentration is visible in Figure 5, suggesting a significant role for deposition and resuspension, which may lower the organic content as it is lost after deposition (Eisma and Kalf, 1987b).

Besides the significance of deposition and resuspension, we also found a strong horizontal variability (Figure 4), a temporal variability during a tidal cycle (Figure 5), and an effect of vertical stratification in the spread of SPM through the water column (Figure 4, right panels). All this suggests that the East Anglian plume is not a plume in the common sense of the word, as if it

were a kind of permanent feature, a 'river' of SPM going steadily from west to east. Its position is also less permanent than coastal pathways of SPM or fine sediments (e.g., van Alphen (1990)), because it is not guided by a coastal closed boundary and ROFIs.

6. Conclusion

We have reported on detailed in-situ measurements at two transects across the East Anglian plume. Through repeated visits to selected stations during a tidal period, we have investigated the intra-tidal variability. Since the plume lies in a frontal area, the advection of the front also shifts the stratified and mixed layers in a transverse (i.e., more or less south-north) direction. This effect was stronger at transect T1 (in the central North Sea) than at T2 (more towards the German Bight) because of the changes in polarization of the tidal current (more circular at T1, whereas at T2 the tidal current was rather rectilinear in the along-plume direction). The character of the front also changes between the two transects, the warmer more saline water was found at the south of T1 but more to the middle (and less pronounced) at T2.

Within a tidal cycle, for T2, we observe higher near-bottom SPM concentrations when currents are high and smaller ones around slack tides, but this pattern is absent from T1 because of the near-circular polarization of the tidal currents, so that effectively slacks never occur.

At T2, we find lower concentrations in our in-situ measurements, typically about 12 mg/l (median value for T2 in Fig. 3), compared to T1 (median value at T1 is 18 mg/l in Fig. 3). On the other hand, neither in the in-situ

measurements nor in the remote-sensing images do we see a clear broadening of the plume, which brings into question whether the East Anglian plume can be regarded as a continuous flow of SPM.

As we have simultaneously measured current profiles and optical backscatter profiles, we are able to deduce the instantaneous transports of SPM throughout the water column, and also the integrated values over a tidal cycle, as well as integrated over depth and along the transect. This produces an estimated net transport of SPM of 13 ($\pm$4) million kg over a full tidal cycle, in the along-plume direction.

The selection of our transects was based on images of optical remote sensing from a day prior to the cruise. We have compared our measurements with four images of near-surface concentrations (based on NIR routine), one prior to the cruise and the others during measurements of transect T2. We have made a detailed comparison for cases in which we have a close correspondence in space and time between the measurements. The spatial trend (i.e., along the transect) agrees well, but in-situ near-surface values are about two times larger than those estimated from remote sensing.

Acknowledgements: We thank Piet Ruardij and the two reviewers for helpful remarks and criticism. Additionally, we thank all onboard the R/V Pelagia as well as the technical support team at NIOZ. This cruise was part of the FOKUZ project.

Bale, A. J., Morris, A. W., 1998. Organic carbon in suspended particulate material in the North Sea: effect of mixing resuspended and background particles. Cont. Shelf Res. 18, 1333–1345.

Capuzzo, E., Stephens, D., Silva, T., Barry, J., Forster, R. M., 2015. Decrease in water clarity of the southern and central North Sea during the 20th century. Global Change Biol. 21, 2206–2214.

Creutzberg, F., Postma, H., 1979. An experimental approach to the distribution of mud in the southern North Sea. Neth. J. Sea Res. 13, 99–116.

de Jonge, V. N., de Jong, D. J., 2002. 'Global Change' impact of interannual variation in water discharge as a driving factor to dredging and spoil disposal in the river Rhine system and of turbidity in the Wadden Sea. Estuar. Coastal Shelf Sci. 55, 969–991.

Downing, J., 2006. Twenty-five years with obs sensors: the good, the bad, and the ugly. Cont. Shelf Res. 26, 2299–2318.

Duran-Matute, M., Gerkema, T., 2015. Calculating residual flows through a multiple-inlet system: the conundrum of the tidal period. Ocean Dyn. 65, 1461–1475.

Dyer, K., Moffat, T., 1998. Fluxes of suspended matter in the East Anglian plume Southern North Sea. Cont. Shelf Res. 18, 1311–1331.

Eisma, D., 1987. The North Sea: an overview. Phil. Trans. R. Soc. Lond. B 316, 461–485.

Eisma, D., Kalf, J., 1987a. Dispersal, concentration and deposition of suspended matter in the North Sea. J. Geol. Soc. London 144, 161–178.

Eisma, D., Kalf, J., 1987b. Distribution, organic content and particle size of suspended matter in the North Sea. Neth. J. Sea Res. 21, 265–285.

579 Eleveld, M. A., Pasterkamp, R., van der Woerd, H. J., Pietrzak, J. D., 2008.
580 Remotely sensed seasonality in the spatial distribution of sea-surface sus-
581 pended particulate matter in the southern North Sea. Est. Coast. Shelf
582 Sci. 80, 103–113.

583 Fettweis, M. P., Nechad, B., 2011. Evaluation of in situ and remote sens-
584 ing sampling methods for SPM concentrations, Belgian continental shelf
585 (southern North Sea). Ocean Dyn. 61, 157–171.

586 Hill, A., Brown, J., Fernand, L., Holt, J., Horsburgh, K. J., Proctor, R.,
587 Raine, R., Turrell, W. R., 2008. Thermohaline circulation of shallow tidal
588 seas. Geopgys. Res. Lett 35, L11605.

589 Lee (ed.), Z. P., 2006. Remote Sensing of Inherent Optical Properties: Fun-
590 damentals, Tests of Algorithms, and Applications. Reports of the Inter-
591 national Ocean-Colour Coordinating Group, No. 5. IOCCG, Dartmouth,
592 Canada.

593 Nauw, J., de Haas, H., Rehder, G., 2015. A review of oceanographic and
594 meteorological controls on the North Sea circulation and hydrodynamics
595 with a view to the fate of North Sea methane from well site 22/4b and
596 other seabed sources. Marine and Petroleum Geology 68b, 861–882.

597 Nechad, B., Ruddick, K., Park, Y., 2010. Calibration and validation of a
598 generic multisensor algorithm for mapping of total suspended matter in
599 turbid waters. Remote Sens. Environ. 114 (4), 854–866.

600 Otto, L., Zimmerman, J. T. F., Furnes, G. K., Mork, M., Saetre, R., Becker,

601 G., 1990. Review of the physical oceanography of the North Sea. Neth. J.
602 Sea Res. 26, 161–238.

603 Pietrzak, J. D., de Boer, G. J., Eleveld, M. A., 2011. Mechanisms controlling
604 the intra-annual mesoscale variability of SST and SPM in the southern
605 North Sea. Cont. Shelf Res. 31, 594–610.

606 Pingree, R. D., Holligan, P. M., Mardell, G. T., 1978. The effects of vertical
607 stability onphytoplankton distributions in the summer on the northwest
608 European Shelf. Deep-Sea Res. 25, 1011–1028.

609 Stanev, E. V., Dobrynin, M., Pleskachevsky, A., Grayek, S., Guenther, H.,
610 2009. Bed shear stress in the southern North Sea as an important driver
611 for suspended sediment dynamics. Ocean Dyn. 59 (2), 183–194.

612 Tiessen, M. C. H., 2013. Cruise report FOKUZ cruise 64PE365. NIOZ, Texel,
613 Netherlands.

614 Tilstone, G. H., Peters, S. W. M., van der Woerd, H., Eleveld, M. A., Rud-
615 dick, K., Schonfeld, W., Krasemann, H., Martinez-Vicente, V., Blondeau-
616 Patissier, D., Rottgers, R., Sorensen, K., Jorgensen, P. V., Shutler, J.,
617 2012. Variability in specific-absorption properties and their use in a semi-
618 analytical ocean color algorithm for MERIS in North Sea and Western
619 English Channel Coastal Waters. Remote Sens. Environ. 118, 320–338.

620 van Alphen, J. S. L. J., 1990. A mud balance for Belgian-Dutch coastal waters
621 between 1969-1986. Neth. J. Sea Res. 25, 29–30.

622 van Leeuwen, S., Tett, P., Mills, D., van der Molen, J., 2015. Stratified and

nonstratified areas in the north sea: Long-term variability and biological and policy implications. J. Geophys. Res. 120, 4670–4686.

7. Figures

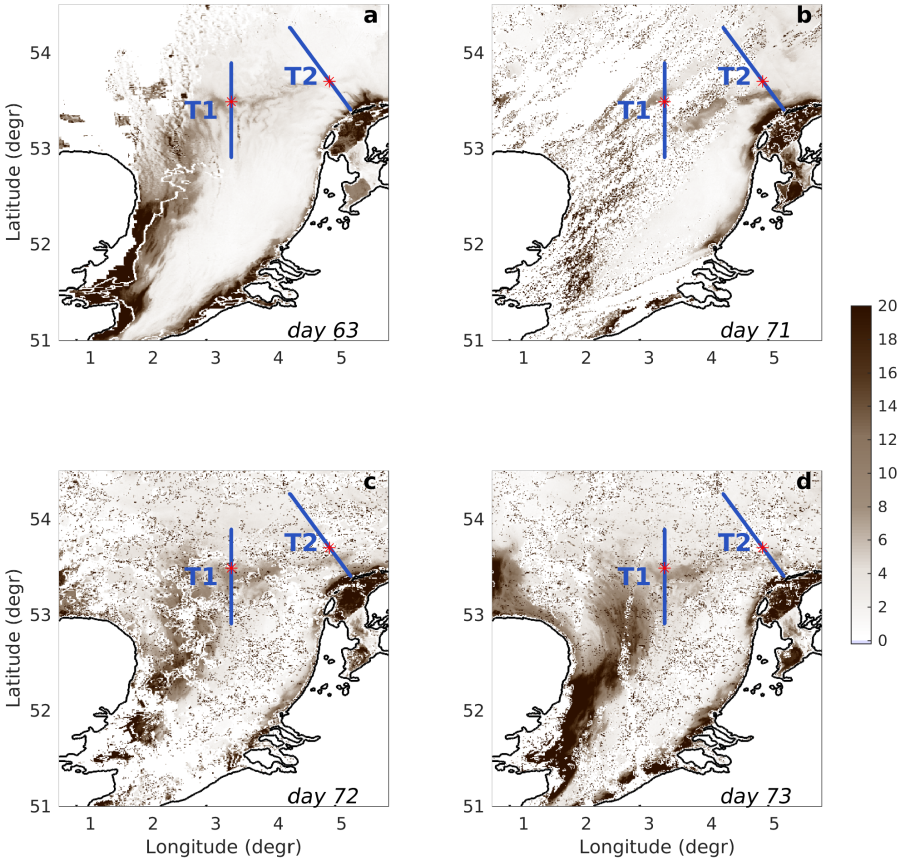

Fig 1: Map of the southern North Sea with the transects T1 and T2 along which in-situ measurements on the transport of SPM were made, during days 66-73, 2013. Also shown are images of estimated surface SPM concentrations

(in mg/l) based on remote sensing. They are from four different days: a) before and b-d) during the cruise.

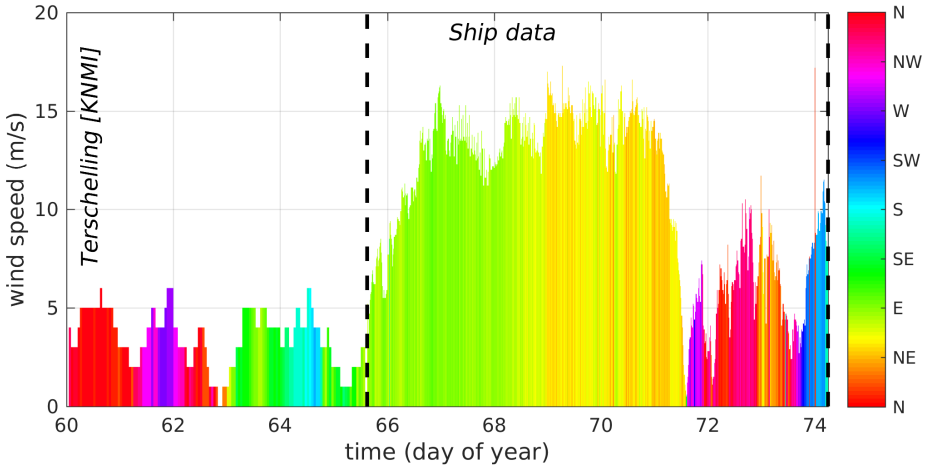

Fig. 2: Wind conditions prior and during the cruise. The vertical indicates the wind speed in m/s, the colour indicates the wind direction (i.e. the direction from which the wind blows).

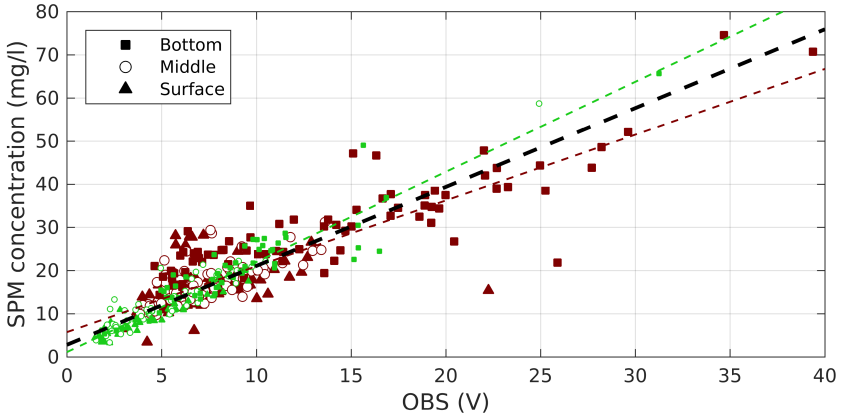

Fig. 3: Relation between OBS values and SPM concentrations, from samples taken from the surface, the bottom, or halfway down the water column. Values from transect T1 are in brown, from T2 in green. The linear

fit (dashed line) is based on a Theil-Sen method applied to all data together.

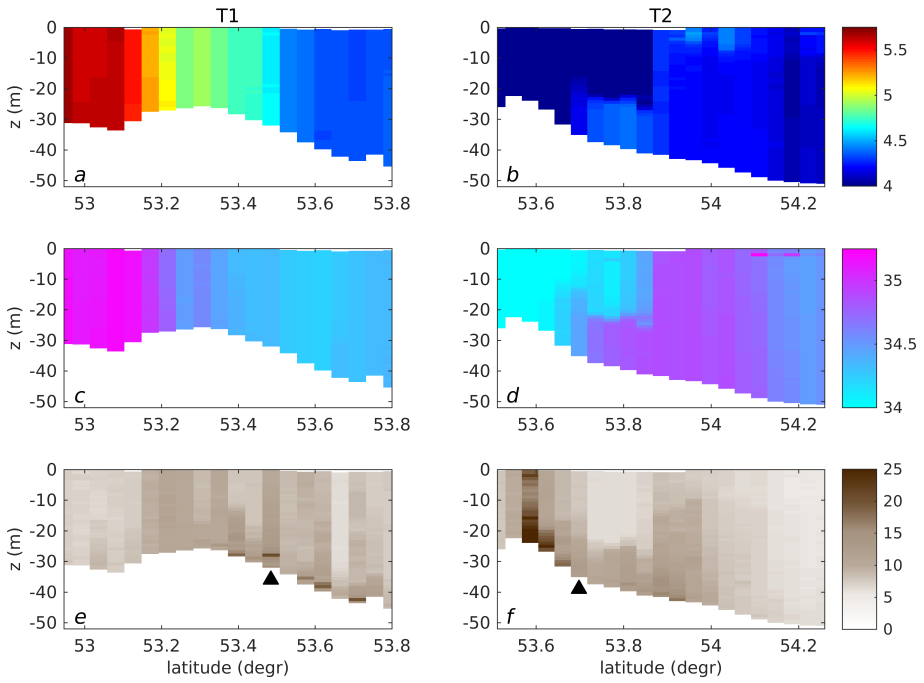

Fig. 4: Results from the full transects. *Left panels:* T1 on 7 March (day of year 66). *Right panels:* T2 on 12 March (day of year 71). Panels a,b) temperature (°C); c,d) salinity (PSU); e,f) SPM concentration (mg/l). Triangles indicate the stations used in Figs 5 and 6.

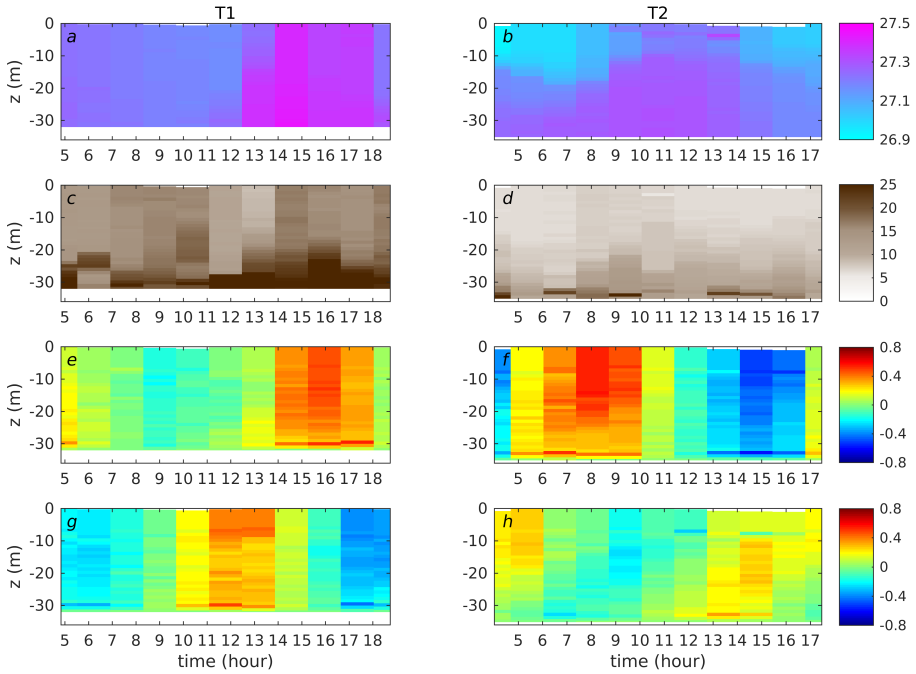

Fig. 5: Results from a full tidal cycle at two stations. *Left panels:* T1, station at 53°29.1′N 3°15.0′E on 8 March (day of year 67). *Right panels:* T2, station at 53°41.9′N 4°48.8′E on 14 March (day of year 73). Panels a,b) density anomaly (kg/m^3); c,d) SPM concentration (mg/l); e,f) current velocity along the plume (i.e., normal to the transect), in m/s, with positive values indicating eastward (left panels) or northeastward (right panels) flows; g,h) current velocity across the plume (i.e., along the transect), in m/s, with positive values indicating northward (left panels) or northwestward (right panels) flows. Time is in UTC.

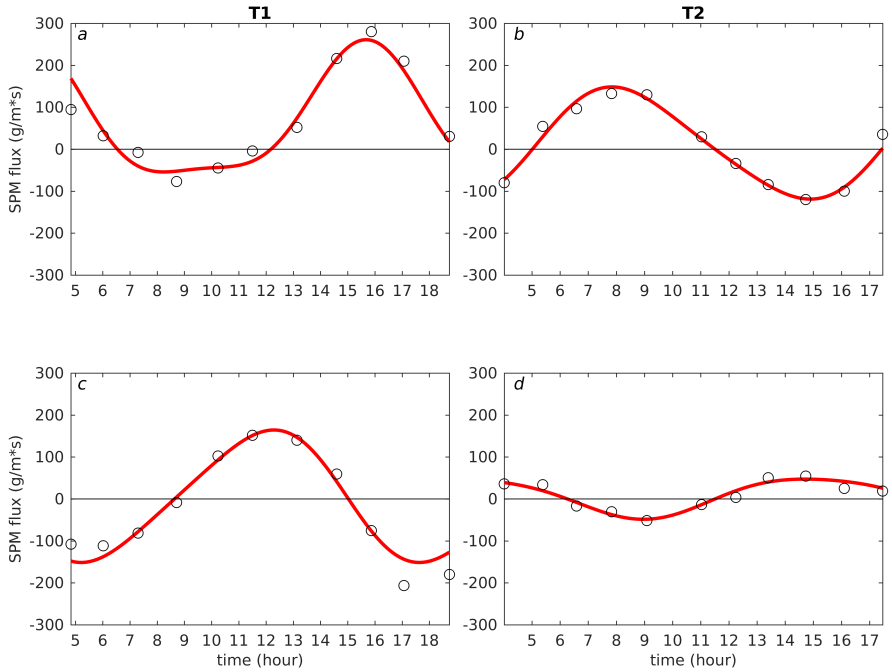

Fig. 6: Depth integrated transports of SPM, indicated by open circles, at the same stations as in Fig. 5, for a,b) the along-plume direction, and c,d) the cross-plume direction. Red lines indicate a harmonic fit based on semidiurnal, quarterdiurnal and residual constituents.

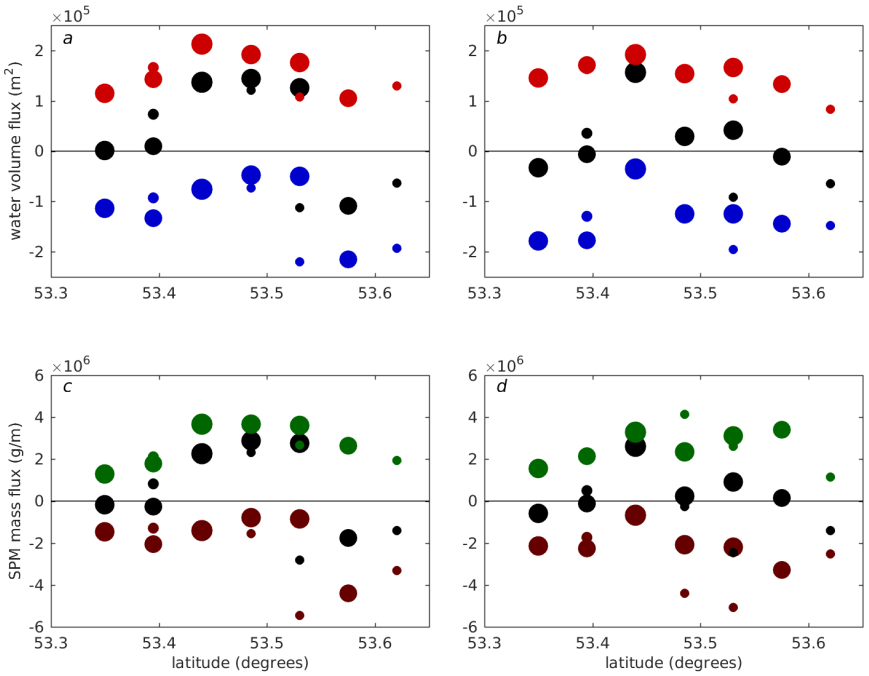

Fig. 7: Depth-integrated transports, integrated over a full tidal cycle: a,b) water; c,d) SPM. Each panel contains the results from seven stations along transect T1. Panels a and c are for the along-plume direction; panels b and d, for the cross-plume direction. Besides the net transport (in black), also the gross transports during flood (positive) and ebb (negative) are indicated, in red and blue, respectively. The size of the circles represents the number of visits that occurred during a 14-hour period, which ranged from 5 (small) to 12 (big).

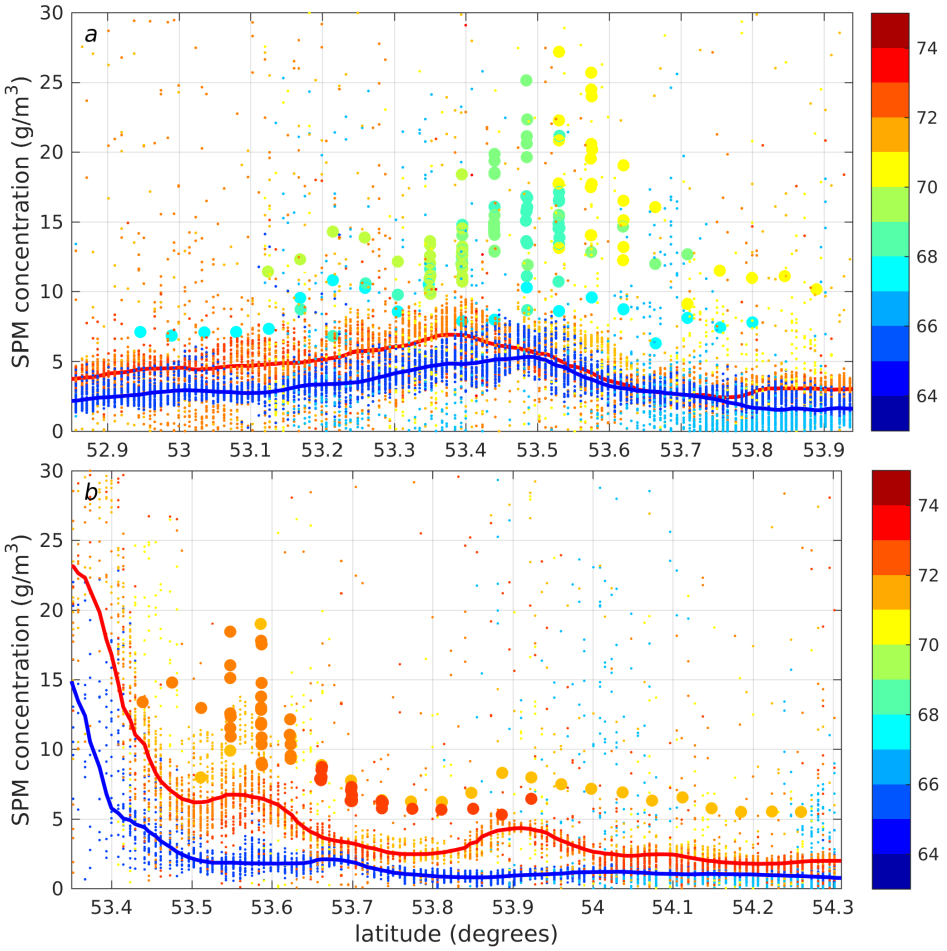

Fig. 8: Comparison between satellite-derived and in-situ measured near-surface SPM concentrations: a) transect T1; b) transect T2. The data based on remote sensing in the vicinity of the stations are shown as small dots. Median values of pre- and post-storm conditions are indicated as the blue (prior) and red (post storm) lines. The in-situ measured SPM concentrations are shown as full circles. Colours indicate day numbers.